

## Cu and Ag deposition on layered *p*-type WSe<sub>2</sub>: Approaching the Schottky limit

W. Jaegermann, C. Pettenkofer, and B. A. Parkinson\*

*Hahn-Meitner-Institut, Abteilung Solare Energetik, Glienickerstrasse 100, 1000 Berlin 39, West Germany*

(Received 8 June 1990)

The interaction of Cu and Ag on the van der Waals (0001) face of *p*-type WSe<sub>2</sub> has been investigated in relation to Schottky-barrier formation and Schottky solar cells using x-ray and uv photoelectron spectroscopy (XPS,UPS), low-energy electron diffraction (LEED), and surface photovoltage measurements. XPS and UPS results show the growth of a metallic overlayer for small coverages without detectable formation of any interfacial reaction layer. In addition, the LEED experiments indicate epitaxially grown (111) metal layers in the form of clusters. Therefore, we conclude that an atomically abrupt interface between the semiconductor and the *M*(111) overlayers is formed. The observed band bending obtained from binding-energy shifts corresponds to the work-function difference following the Schottky-Mott theory. However, the surface photovoltage measured at 300 and 100 K is not in good correspondence to the thermionic-emission model of Schottky barriers. Therefore, an alternative interface model is suggested considering *n*-type doping of the semiconductor interface due to intercalation of the adsorbed metal atoms.

### INTRODUCTION

The interplay between interface interactions and electronic barriers at semiconductor-metal junctions is still the subject of intense studies.<sup>1-3</sup> The magnitude of the electronic barrier  $\phi_B$  formed at the interface scatters between the extremes of the Schottky limit ( $\phi_B = \phi_M - \chi_{sc}$ ) (Ref. 4) and the Bardeen limit [ $\phi_B = S(\phi_M - \chi_{sc}) + \phi_0$  with  $S$  approaching 0].<sup>5</sup> A relation between the chemical nature of the semiconductor (electronegativity difference  $\Delta\chi$  of constituent elements) and  $S$  suggests that the type of surface interactions plays an important role. A more ideal behavior ( $S=1$ ) is observed for ionic semiconductors (a closer relation to the Schottky limit) and a higher tendency to Fermi-level pinning ( $S=0$ ) for covalent semiconductors (closer relation to the Bardeen limit) with a sharp transition point between the two extreme cases at  $\Delta\chi=0.7-0.8$ .<sup>6,7</sup>

Surface-science techniques have been used to elucidate the microscopic details of the semiconductor-metal interface formation and to determine the decisive factors for the barrier height. The results indicate that the "interphase" may be considerably complex in both structure and composition and usually depends on the chemistry of the semiconductor-metal combination.<sup>1-3,8,9</sup> For this reason there are still different theoretical models discussed in the literature to account for the observed experimental facts of nonideal Schottky-barrier heights. The original model of Bardeen attributes the pinning effect to intrinsic surface states of clean semiconductor surfaces.<sup>5</sup> In more recent models extrinsic surface states resulting from the interaction to the contact metal are favored. In the defect model the interfacial pinning states are due to near-surface lattice defects induced by the deposited contact metal which only reflect the intrinsic bulk properties of the semiconductor.<sup>9,10</sup> In the metal-induced-gap-states (MIGS) model the surface states result from the penetration of metal electron states into the semiconductor band

gap.<sup>11-14</sup> An interfacial reaction layer creating interface states responsible for Fermi-level pinning is also discussed as a model for strongly reacting semiconductor-metal combinations.<sup>15</sup> A general unified model combining the theoretical approaches is suggested for group-IV and III-V semiconductors<sup>10,15-17</sup> but may not be appropriate for semiconductor compounds of completely different chemical character.

Layered metal chalcogenide semiconductors may be considered to be ideal model systems for the investigation of fundamental aspects of semiconductor-metal interactions. The structure of these compounds is characterized by lamellar sheets of covalently bound two-dimensional sandwich-like subunits which are separated from each other by weak so-called van der Waals interactions. The crystals can easily be cleaved across this van der Waals gap leading to chemically saturated, hexagonally close-packed chalcogenide layers. The chemical inertness of the obtained basal plane [(0001) face] due to the lack of dangling bonds has already been demonstrated in a number of surface studies with a variety of adsorbates.<sup>18-20</sup> Also the adsorption of metals has increasingly been investigated on clean (0001) surfaces.<sup>21-31</sup> It was shown that the deposited metal in some cases may intercalate, resulting in a bulk reaction with the semiconductor,<sup>26,30,31</sup> or a reaction at the semiconductor surface leads to the formation of a new surface phase.<sup>21-24,27,29</sup> In those cases where surface reactions have not been observed,  $\Phi_B$  has been quoted to follow the Schottky limit.<sup>21,22,24,25,27</sup> The group-VIB dichalcogenides (such as MoS<sub>2</sub> or WS<sub>2</sub>) are especially inert towards interfacial reactions with many metal adsorbates.<sup>24,25,27</sup> An atomically abrupt interface is reported between the semiconductor substrate and epitaxially grown (111) layers of group-IB metals.<sup>8</sup> For these semiconductors the electronegativity difference is in the range of 0.8 to 0.6 (Ref. 32) just passing the transition point to Fermi-level pinning. In some of the previously reported studies, semiconductor-metal combinations have

been used, for which strong band bending is not expected. Because of the larger work-function differences we extended our studies to *p*-type  $\text{WSe}_2$  and used Cu and Ag as contact metals. The surface, cleaved in UHV, and changes induced by deposited metals were analyzed by UV and x-ray photoelectron spectroscopy (UPS, XPS), low-energy electron diffraction (LEED), and *in situ* surface photovoltage experiments. The saturation surface photovoltage is an important quantity as *p*-type  $\text{WSe}_2$  is considered as a promising material for Schottky solar cells.<sup>33</sup> The electrically determined character of the barrier, however, is far from ideality concerning photovoltage and diode current-voltage behavior, which leads to rather low-energy conversion yields below 2%.<sup>33</sup> In this study we also want to analyze whether the low conversion yields are due to intrinsic problems of the interface or to problems of barrier preparation that might be improved.

### EXPERIMENT

The experiments were performed in a commercial UHV-multitechnique system (VG ESCALAB Mk II). The base pressure of the system is  $5 \times 10^{-11}$  torr in the analyzer chamber and  $3 \times 10^{-10}$  torr in the preparation chamber. Cleaved layered crystals remain uncontaminated during more than 48 h as judged from UP spectra. Mg  $K\alpha$  for XPS and He I and He II for UPS measurements are used as excitation sources. The spectrometer calibration was continuously checked with polycrystalline sputtered Cu after certain sets of experiments. If not otherwise specified the photoelectrons are detected normal to the probed surface. For UP spectra the sample was biased negatively by 2.0 V to ensure correct values for the work function from the secondary electron onset. LEED experiments were performed by a reverse-view LEED system (VSW).

Single crystalline Nb-doped *p*-type samples of  $\text{WSe}_2$  were prepared by gas transport reaction and are of typical dimensions  $5 \times 5 \times 0.2$  mm.<sup>34</sup> The doping density is determined as about  $10^{17}$  cm<sup>-3</sup> from Hall measurements. They were mounted with one van der Waals plane by Ag epoxy for a sufficiently conductive back contact. This procedure allows the use of the semiconductor bulk Fermi level  $E_F$  as the reference for the binding-energy scale. The results are not changed when Pt or Au paste was used for the Ohmic back contact. Band bending or double layer potential shifts due to metal adsorbates are given as shifts of core and valence level binding energies  $E_B$  with respect to  $E_B = 0$  equivalent to  $E_F$ . Surface photovoltages were measured from shifts of the photoemission distribution curves due to white bias light (W/Hal, 100 mW/cm<sup>2</sup>). The obtained light-induced shifts are perfectly reversible indicating that only a redistribution of electronic charge carriers at the interface is involved. No evident effect is observed due to He excitation<sup>35</sup> as checked by intensity variation; however, small differences (0.05 eV) are observed in binding-energy shifts and/or surface photovoltages between He I and He II excitation. A decrease of sample temperature to 100 K, which should reduce possible recombination losses and there-

fore increase the surface photovoltage effect, did not change the measured photovoltages.

Cleaving in UHV was performed by thin Ni foil attached to the second basal plane of the crystal which was removed by a wobble stick. By this procedure perfectly smooth van der Waals (0001) surfaces can be prepared. Cu and Ag was deposited *in situ* onto the cleaved surfaces from a resistivity heated metal sublimation source. All metal coverages are expressed herein in deposition times  $t_d$  (sec). The deposition rate was estimated by XPS with different exposure times. The core-level intensities used were corrected by theoretical photoionization cross sections.<sup>36</sup> One monolayer of Cu corresponds roughly to a deposition time of 100 sec.

### RESULTS

#### Cu deposition on *p*-type $\text{WSe}_2$

In Figs. 1 and 2 the He I and He II spectra of *p*-type  $\text{WSe}_2$  in the course of Cu deposition are summarized. The spectral features measured for the clean  $\text{WSe}_2$ (0001) surfaces correspond to published spectra.<sup>37,38</sup> A steep valence-band photoemission onset is observed for different samples at  $E_B = 0.4 \pm 0.1$  eV with a weak emission tail up to  $E_B = 0.2$  eV in reasonable correspondence to the *p*-type conductivity of the samples. The valence-band maximum is expected at  $\Gamma$  according to band-structure calculations.<sup>38</sup> Photoemission experiments along  $\Gamma-A$  (normal to the van der Waals plane) with variation of excitation energy show strong dispersion of the emission peaks and also of the intensity of the emission onset around 0.2 eV. The work function determined

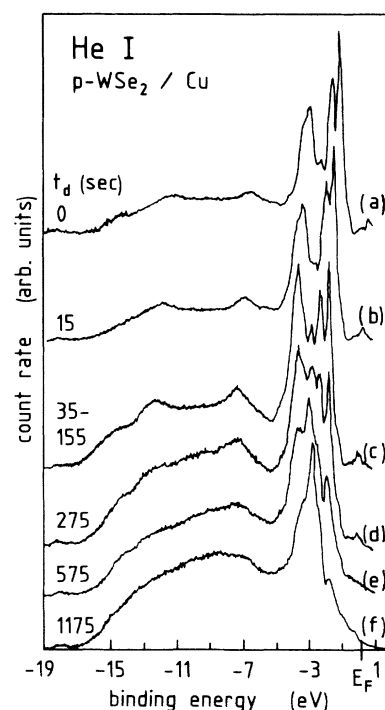


FIG. 1. He I UP spectra of *p*-type  $\text{WSe}_2$ (0001) in the course of Cu deposition.

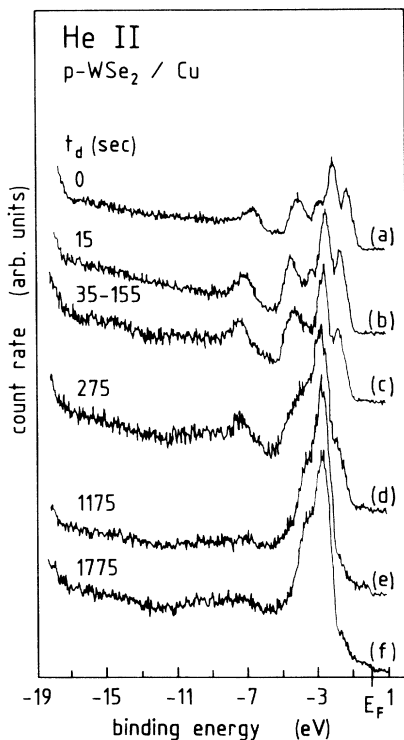


FIG. 2. He II UP spectra of *p*-type WSe<sub>2</sub>(0001) in the course of Cu deposition.

from the secondary electron emission onset ranges for different samples from values about 5.6 eV (used in this experiment) to values of 5.0 eV.

Deposition of very small Cu coverages ( $t_d = 15$  sec) already leads to a pronounced shift of the energy distribution curve (EDC) of 0.4 eV towards increased binding energies (away from  $E_F$ ). In this coverage regime the contribution of the Cu 3*d* emission in the UP spectra is submerged in the Se 4*p* emission of WSe<sub>2</sub> and only a tiny Cu 2*p* core-level peak can be measured in the XP spectra. The estimation of coverage is below 0.1 ML, which is already sufficient to disturb the electronic distribution at the interface. Further deposition of Cu increases the binding-energy shift to a maximum value of 0.75 eV at  $t_d = 55$  sec. The changes of the binding energies with respect to  $E_F$  in the course of Cu deposition are more clearly shown in Fig. 3. For this plot the binding-energy shifts of the first intense emission has been used which can be followed in the He I and He II spectra up to high Cu coverages. After the initial increase a gradual decrease of binding energy is observed for higher Cu doses saturating at a value of about 0.6 eV.

For increasing coverages of Cu ( $t_d > 60$  sec), an increasing contribution of Cu 3*d* emissions can be observed in the spectra. Also a Fermi edge develops, proving conclusively that Cu is growing as a metallic overlayer. At high coverages ( $t_d > 395$  sec for He II and  $t_d > 875$  sec for He I) the spectra closely correspond to normal emission spectra of the (111) surface of metallic Cu. Difference spectra obtained from spectra of smaller coverages (Fig. 4) are characterized by a negative contribution of the

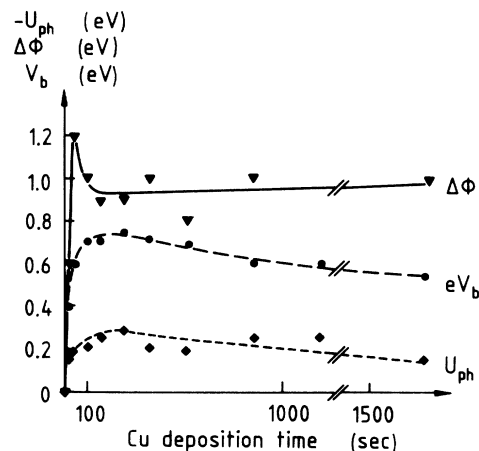


FIG. 3. Changes of band bending (binding energy)  $V_b$ , work function  $\Delta\Phi$ , and surface photovoltage  $U_{ph}$  in the course of Cu deposition.

pure WSe<sub>2</sub> EDC and a positive contribution of Cu 3*d* emission, which is identical to the spectra of the metallic overlayer observed at high coverages. In addition, in the difference spectra the Fermi edge is clearly resolved already at small Cu coverages. These data indicate that the metallic overlayer is already formed at small coverages and that a surface reaction layer can be excluded in correspondence to previously published results on similar compounds.<sup>21-27</sup>

The shift of the EDC can partly be removed by bias light creating a maximum surface photovoltage of 0.3 eV. This bias light effect is perfectly reversible and shifts the spectra backward and forward upon illumination (see Fig. 5). It is clearly observed in the UP spectra with He I and He II excitation and to a lesser extent in the XP spectra (which may be due to lower surface sensitivity). The changes of surface photovoltage with Cu coverage are also plotted in Fig. 3. In addition the work-function change  $\Delta\Phi$ , determined from the secondary electron onset, is shown in dependence of Cu coverage. It should be noted that the determination of the work function from the secondary onset leads to rather large errors (about 0.2 eV) as a pronounced sharp cutoff is often not obtained. In addition the cutoff is evidently composed of at least two contributions at higher Cu coverages ( $t_d > 55$  sec), one of which ( $\Phi = 5.0$  eV) is attributed to Cu(111).

The binding-energy shifts due to the deposited metal also appear in the XP spectra. Its value of about 0.3 eV, however, is considerably smaller. Pronounced changes of spectral features are not observed in the course of Cu deposition (see Fig. 6). The full width at half maximum (FWHM) of the substrate peaks increases slightly at lower coverages but subsequently decreases again. No changes are observed in the W levels, whereas a slight asymmetry of the Se 4*d* level towards lower binding energies is attributed to the interaction of the surface Se atoms to the Cu overlayer, however the formation of interfacial elemental Se can be excluded. The Cu 2*p* emission lines show binding-energy shifts in the course of Cu deposition from a value of about 933 eV to a value of

932.4 eV, which is typical for bulk Cu. Parallel large FWHM's of typically 2 eV are observed for small Cu coverages which decrease to a final value of 1.2 eV for the thick metal overlayers. The changes of peak intensities with Cu deposition time are plotted in Fig. 7. The Cu-to-W intensity ratio shows a nearly linear increase with a small slope at low coverages below  $t_d=55$  sec and a

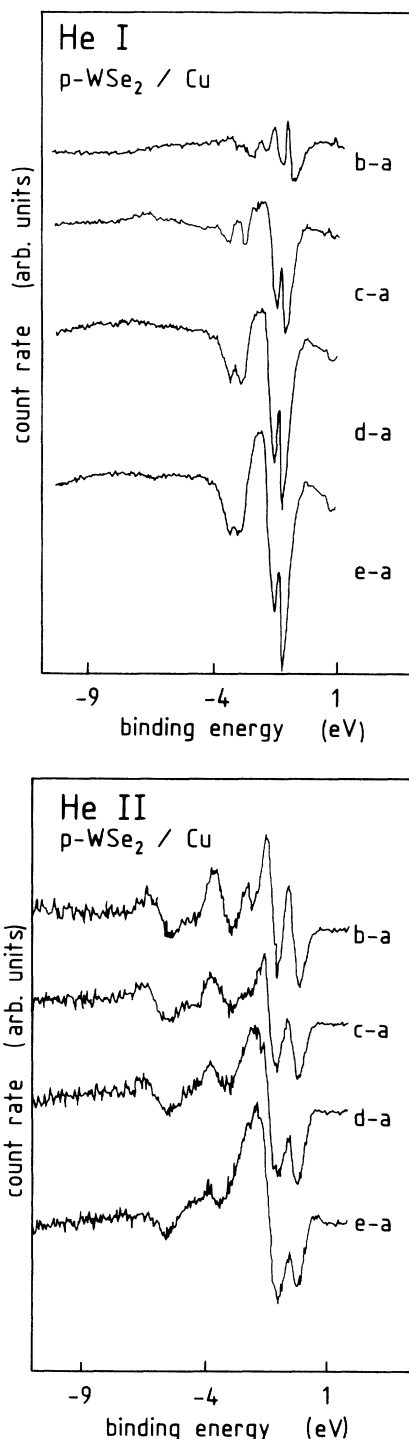


FIG. 4. He I and He II UP difference spectra in the course of Cu deposition. The designation is related to Figs. 1 and 2.

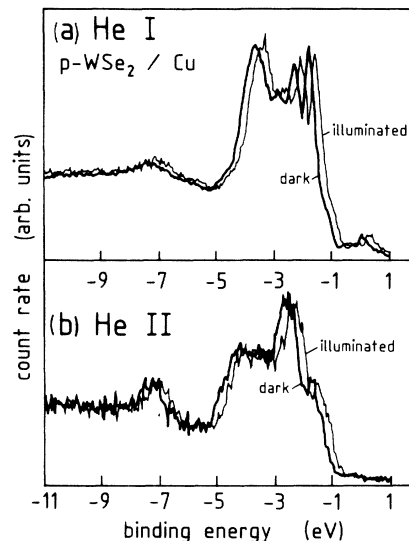


FIG. 5. He I and He II UP spectra ( $t_d=155$  sec) showing the surface photovoltage induced by white bias light ( $\sim 100$  mW/cm<sup>2</sup>).

linear increase with increased slope at higher deposition times. For very high coverages,  $t_d > 5000$  sec, only the signals of the Cu overlayer can be detected. It should be noted that the Se-to-W intensity ratio remains constant and close to the theoretical value of 2.0.

The LEED diffraction patterns included in Fig. 6 also indicate that an epitaxial overlayer of Cu(111) is formed. Up to coverages of about 6 ML ( $t_d=575$  sec) the original LEED spots of the substrate (hexagonal symmetry) dominate without any evidence for a defined overlayer of the deposited Cu. At coverages exceeding  $t_d=875$  sec a second hexagonal diffraction pattern develops, superimposed with the substrate diffractions. The ratio of the reciprocal-lattice constants of 0.77 corresponds to the expected ratio of distances between the WSe<sub>2</sub> lattice constant in the (0001) plane ( $d=3.9$  Å) and the Cu atoms in the (111) plane ( $d=2.55$  Å). At Cu coverages exceeding  $t_d=3000$  sec the substrate diffraction pattern disappears and only the Cu(111) pattern remains.

#### Ag deposition on *p*-type WSe<sub>2</sub>

The results of this system have already been presented in part elsewhere<sup>39</sup> and will only be summarized here for the sake of comparison. Similarly to the Cu case the deposition of Ag leads with increasing coverage to EDC's which are evidently only composed of contributions of the substrate and of a metallic Ag overlayer (see for example the He II spectra of Fig. 8). The Ag emission features closely correspond for both excitation lines (He I and He II) to published spectra of Ag(111) surfaces.<sup>40</sup> No evidence is found for any interfacial reaction layer.

The binding-energy shifts of the spectra (band bending) in the course of Ag deposition are summarized in Fig. 9. The shift reaches a maximum value of 0.95 eV for intermediate Ag doses [Fig. 8(e), equivalent coverage  $\Theta$  of 0.5 ML] and slowly decreases again for high Ag coverages to a saturation value of 0.8 eV. For covered surfaces white

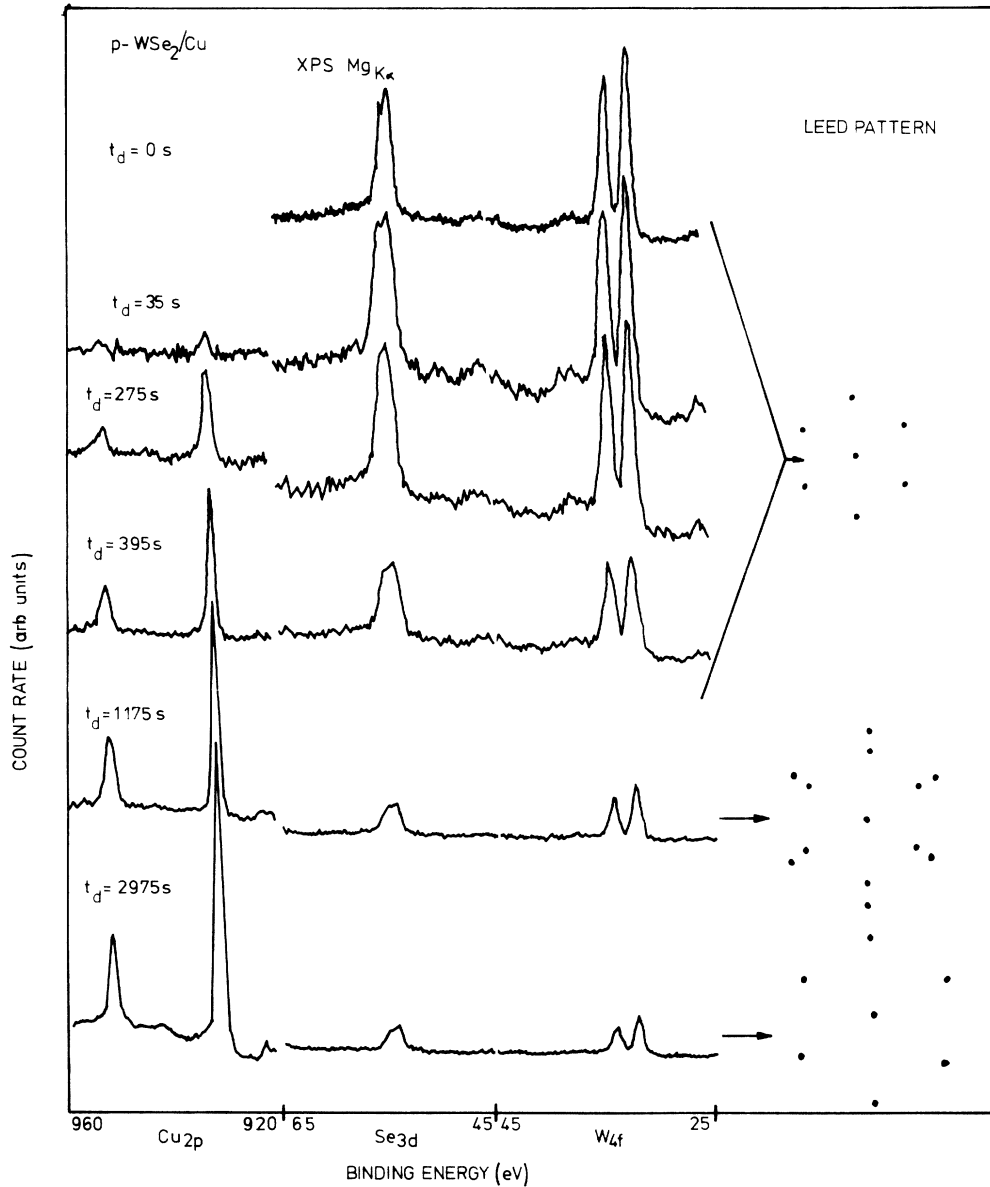


FIG. 6. XP spectra (Mg  $K\alpha$ ) in the course of Cu deposition. The LEED diffraction pattern obtained for different Cu deposition stages is also schematically shown.

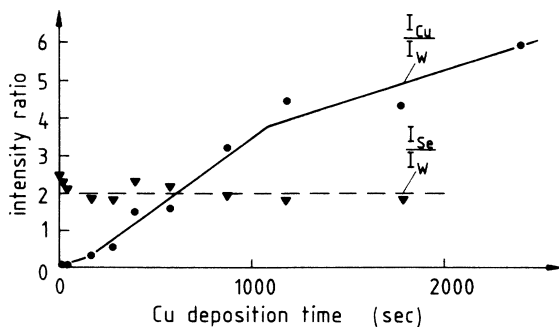


FIG. 7. Changes of Cu-to-W and Se-to-W XPS intensity ratios in the course of Cu deposition.

bias light illumination reduces the Ag-induced binding-energy shift. This surface photovoltage reaches a maximum value of 0.3 eV for intermediate coverages and slowly decreases again at high coverages (see also Fig. 9). It is perfectly reversible, which means that switching the light on and off reproducibly shifts the EDC backward and forward.

An interfacial reaction layer can also be excluded from the XPS data. The substrate emission lines remain unchanged during Ag deposition only showing binding-energy shifts due to band bending. The Ag  $3d_{5/2}$  emission line does not exhibit the pronounced binding-energy shift observed for Cu  $2p$ . Only the FWHM decreases from 1.5 to 1.0 eV. The relative Se-to-W intensity

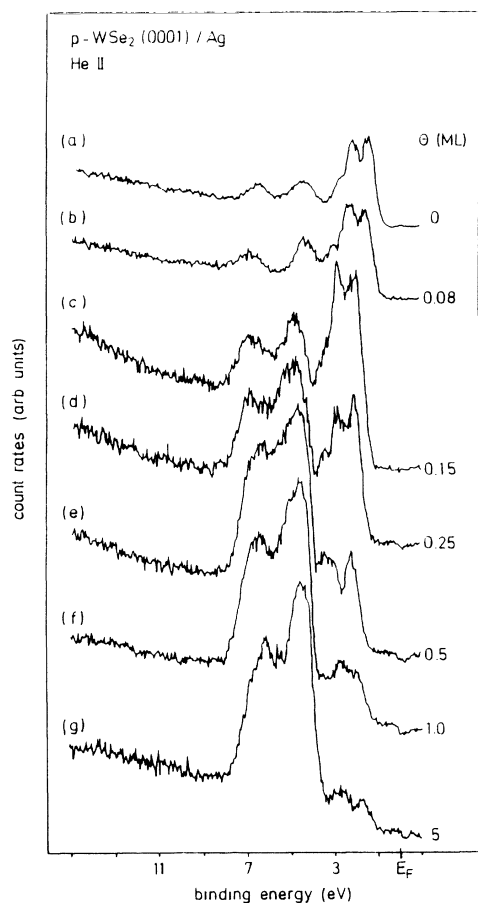


FIG. 8. He II UP spectra in the course of Ag deposition (given as coverage  $\Theta$  in ML).

remains constant in the course of Ag deposition. LEED experiments of the cleaved samples show a sharp hexagonal diffraction pattern on a low background in the energy range of 50 to 150 eV. This diffraction pattern remains unchanged during Ag deposition, indicating that the Ag layer grows epitaxially in (111) orientation in registry with the substrate confirming our UPS data.

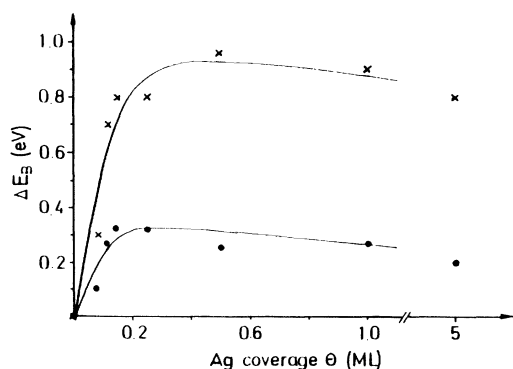


FIG. 9. Binding-energy shift  $\Delta E_B$  ( $\times$ ) and surface photovoltage  $U_{ph}$  ( $\bullet$ ) in dependence on Ag coverage.

## DISCUSSION

### Morphological structure of the interface

Our results indicate that an atomically abrupt semiconductor-metal interface is formed at the  $M/WSe_2$  boundary in correspondence to previously published experiments on comparable semiconductor-metal combinations.<sup>21-27</sup> This conclusion is based on our XPS data but mostly on the more surface-sensitive UP spectra. XP core-level spectra might hide surface reactions when the chemical shifts of the elements in the formed phases do not differ too much. However, we do not find any changes of emission intensity ratios in the course of metal deposition, which usually are obtained for surface exchange reaction and subsequent enrichment of substrate elements in the deposited metal layer. Segregation and allowing processes which are of importance for many semiconductor-metal interfaces<sup>1-3</sup> can evidently be excluded. The UP spectra and even more the difference spectra clearly indicate that interfacial reaction layers do not show up and that the spectra for all coverages are composed of a superposition of the  $WSe_2$  EDC and the EDC of a metallic (111) overlayer.

Our LEED results prove that the metallic overlayer is growing as an epitaxial (111) layer onto the hexagonal substrate formed by the Se atoms. This growth process is induced by the atomic flatness of the hexagonally close-packed substrate, which favors the growth of the close-packed (111) crystal plane of the fcc lattice of Cu and Ag. The coverage dependence of the LEED patterns showing unchanged substrate patterns at an equivalent metal coverage exceeding some monolayers and the superposition of substrate diffraction and metal overlayer diffraction spots at higher metal coverages suggest that the Cu overlayer is evidently deposited in the form of clusters corresponding to the Volmer-Weber growth mode reported in the literature for weak substrate-overlayer interaction.<sup>41</sup> The Ag deposits seem to interact more strongly, as in most cases unchanged diffraction patterns are observed for all metal coverages. The different growth processes which might be found are more thoroughly investigated for  $WS_2$ ,  $MoTe_2$ , and  $WTe_2$  van der Waals surfaces with different group-IB elements.<sup>42</sup> Also in this work it was reported that deposited Cu is less strongly interacting than Au and Ag and the Volmer-Weber growth mode was quoted. However, we observed that the metal overlayer growth mode is very much dependent on the experimental parameters such as, e.g., deposition rate and surface quality.

Summarizing, the morphology of the  $WSe_2/Cu, Ag$  interface as determined in our experiments corresponds to an ideal semiconductor-metal interface with an atomically abrupt boundary between a hexagonal close-packed semiconductor substrate and single crystalline islands of a (111)-oriented fcc metal overlayer.

### Electronic barrier at the interface

Based on the ideal morphology of the interface the electronic barrier formed should give conclusive experimental evidence for the validity of the different theories

of Schottky-barrier formation for this special kind of semiconductor substrate. If we take the binding-energy shift induced by the deposited metal as a measure of the induced band bending, the barrier closely corresponds to the Schottky limit. A schematic sketch of the energy diagram is shown in Fig. 10. It is based on a work function of 5.6 eV, a band gap of 1.2 eV,<sup>43</sup> and a difference  $E_F - E_V$  of 0.2 (taken from the photoemission data). This difference is calculated as 0.1 eV from the doping density. We do not think that this discrepancy is related to deviations from flatband positions as no photovoltage is observed for the cleaved surfaces. In addition we observed for *n*-type samples a difference  $E_F - E_V$  of 1 eV.<sup>44</sup> The energetic positions also agree well to flat band potentials measured for *n*-type WSe<sub>2</sub> [ $E_{fb} = 0.0$  V versus normal hydrogen electrode (NHE)] and *p*-type WSe<sub>2</sub> ( $E_{fb} \approx +0.5$  V versus NHE) in electrochemical junctions<sup>45</sup> (the relation between the absolute scale related to the vacuum level and the electrochemical scale related to the NHE is reported as 4.5 to 4.8 eV (Ref. 46). Based on the above determined position of the Fermi level (work function) in *p*-type WSe<sub>2</sub> and the work function of the deposited *M*(111) layers, a band bending is obtained which follows the semiconductor and metal overlayer work-function difference as expected for the Schottky limit (Table I). In this table also the results of recent studies of Au deposition on *p*-type WSe<sub>2</sub> (Ref. 47), which also forms ideal nonreactive interfaces, are included. The barrier dependence is additionally presented in Fig. 11 showing a plot of band bending versus *M*(111) work function.<sup>48</sup> The obtained experimental values follow a line with slope 1 as expected for the Schottky limit. From this plot an effective work function valid for the barrier formation of 5.6 eV can be derived.

Summarizing, it can be stated that, also based on the binding-energy shifts, an ideal Schottky-type behavior is obtained which agrees to previously reported results on nonreacting layered semiconductor interfaces.<sup>21–27</sup>

TABLE I. Comparison of experimental values for band bending ( $\Delta E_B$ ) and surface photovoltage ( $U_{ph}$ ) with theoretical ones ( $\Phi_{sc} - \Phi_M$ ,  $U'_{ph}$ ).

	$\Phi_M^a$ (eV)	$\Phi_{sc}^b - \Phi_M$ (eV)	$\Delta E_B$ (eV)	$U_{ph}$ (V)	$U'_{ph}^c$ (V)
Cu <sub>max</sub>	4.94	0.7	0.75	0.3	0.42
Cu <sub>sat</sub>	4.94	0.7	0.6	0.2	0.27
Ag <sub>max</sub>	4.74	0.9	0.95	0.3	0.62
Ag <sub>sat</sub>	4.74	0.9	0.8	0.2	0.47
Au <sup>d</sup>	5.31	0.3	0.4	0.15	0.1

<sup>a</sup>*M*(111) face, CRC Handbook (Ref. 48).

<sup>b</sup> $\Phi_{sc} = 5.6$  eV, *p*-type WSe<sub>2</sub>(0001), UHV cleaved.

<sup>c</sup>Calculation based on barrier height  $\Phi_B = \Delta E_B + 0.2$  eV, photocurrent 15 mA/cm<sup>2</sup> (Ref. 29), and Richardson constant 120 A/cm<sup>2</sup> K.

<sup>d</sup>Reference 55.

Especially, results with *n*-type WS<sub>2</sub> show no binding-energy shifts and Cu and Ag and only a small binding-energy shift of 0.3 eV for Au,<sup>27</sup> which also fits the Schottky theory and supports our conclusion.

However, the values obtained for the surface photovoltage effect (Table I) are considerably lower than the band-bending values. They prove to be insensitive to variations of experimental conditions such as light intensity and sample temperature, suggesting that saturation conditions for the photopotential have been reached. In addition, our values are close to the photopotentials reported for Schottky solar cells under the AM1 (where AM denotes air mass) condition.<sup>33</sup> The saturation photovoltage may deviate considerably from band bending when the charge-carrier injection models of solid-state Schottky junctions are applied.<sup>1,49</sup> The applicability to UHV deposited thin metal layers has recently been the subject of controversy.<sup>50</sup> Based on the theoretical expectations of the diode current voltage characteristic of

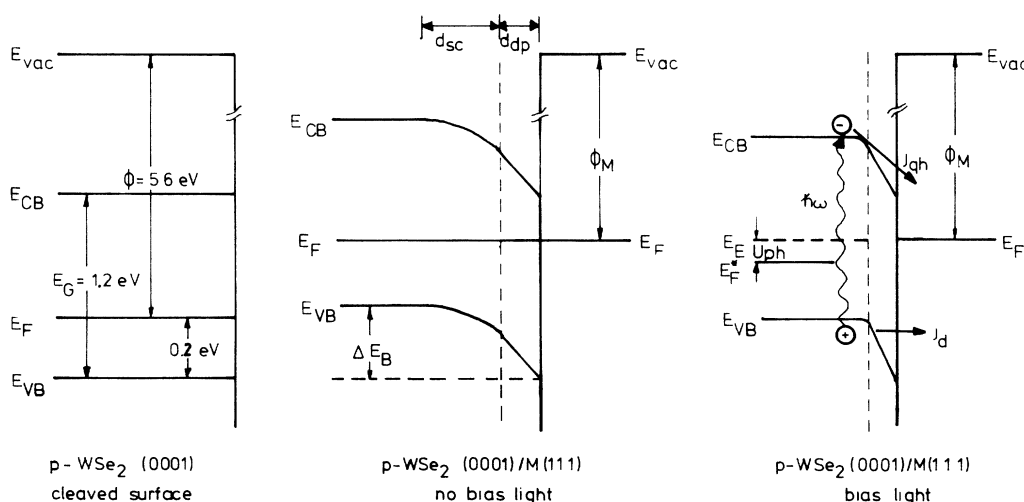


FIG. 10. Schematic energy diagram of the *p*-type WSe<sub>2</sub>(0001) surface (a) after cleavage and (b) after Cu deposition. Details are given in the text.

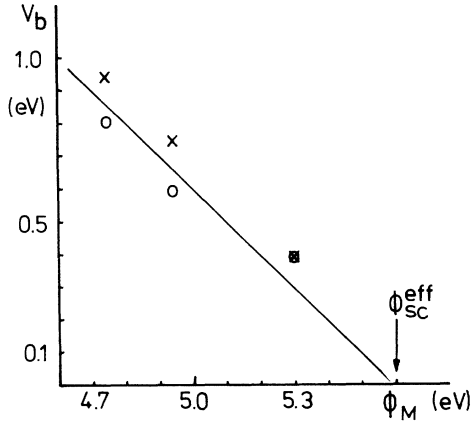


FIG. 11. Binding-energy shifts induced by Cu, Ag, and Au vs metal (111) work function. For Cu and Ag the maximum value ( $\times$ ) and the saturation value ( $\circ$ ) are given (see Figs. 3 and 9) and for Au the saturation value is given (different dependence on metal coverage without maximum).

Schottky barriers, the (photo)current-voltage dependence in the thermionic emission model is given by<sup>1,49</sup>

$$j = j_{ph} - j_d = j_{ph} - j_0 [\exp(-qV/kT) - 1],$$

$$j_0 = AT^2 \exp(-\Phi_B/kT).$$
(1)

For steady-state open circuit condition under illumination,  $j_{ph}$  equals  $j_d$  and  $V$  corresponds to the photovoltage  $V_{ph}$ :

$$V_{ph} = (kT/q) [\ln(j_{ph}/j_0) + 1].$$
(2)

From typical values for the photocurrent  $j_{ph}$  (15 mA/cm<sup>2</sup>),<sup>33,51</sup> barrier heights as obtained in our experiments (Table I), and the Richardson constant  $A$  of 120 A<sup>2</sup>/K<sup>2</sup>cm<sup>2</sup> the photopotentials can be calculated (Table I). It must be noted, however, that this is only a rough estimate since a more precise value of the Richardson constant for the layered materials is not available to us. Nevertheless, the experimental data are considerably below the theoretical ones. In addition, the independence of photovoltage on sample temperature is a puzzling result. The photovoltage should considerably increase approaching the value of band bending for sample temperatures of 100 K, which is not observed experimentally. Therefore, an alternative explanation for the observed data must be considered. It may be possible that small quantities of the deposited metal in dopant concentration are intercalated in the  $p$ -type WSe<sub>2</sub> substrate changing the surface doping to  $n$ -type. We expect that this effect of near surface doping results from diffusion of the deposited metal into the layers from defects and step sites on

the surface. In Fig. 10(b) this effect of doping is schematically indicated by a doping profile at the interface. This part of the barrier contributes to the binding-energy shift but not to the surface photovoltage. It has been shown that the layered materials can possibly intercalate guest atoms<sup>52</sup> also in UHV deposition experiments<sup>26,27,30,31</sup> even if intercalation of Cu in WSe<sub>2</sub> in stoichiometric quantities is not reported.<sup>52</sup> It is not possible to judge based on the reported experiments whether intercalation doping actually occurs, as the doping concentration is well below our detection limit. However, it has been reported that the bulk Fermi level is shifted to  $n$ -type conductivity by doping with Cu.<sup>53</sup> As a consequence, extra electron states are introduced close to the conduction band and near to midgap position, which may be responsible for the low photovoltage. In addition we have shown that UHV deposited Cu can be intercalated into TaS<sub>2</sub> in stoichiometric quantities under similar conditions.<sup>54</sup> Also intercalation of deposited alkali-metal atoms has been observed for layered WX<sub>2</sub> ( $X = S, Se$ ).<sup>30,55</sup>

In summary, ideal Schottky-type behavior is not observed when nonequilibrium conditions, as in photovoltage measurements, are investigated. Our results agree to the nonideal (photo)current-voltage curves obtained for Schottky solar cells based on  $p$ -type WSe<sub>2</sub>.<sup>33</sup> Interfacial reaction layers and related electronic Fermi-level pinning can definitely be excluded as being responsible for nonideality. It seems that band-gap states most probably due to intercalated metal atoms of the metal contact layer drastically influence the nonequilibrium behavior of these types of Schottky junctions.

## SUMMARY AND CONCLUSION

The  $p$ -type WSe<sub>2</sub>/Cu, Ag (Au) interface seems to be an ideal Schottky barrier concerning the morphological structure as well as the band-bending values. We do not see any experimental evidence for a surface reaction. An abrupt interface is formed between the substrate and an epitaxial  $M(111)$  layer. The obtained binding-energy shifts are given by the difference of semiconductor and metal work function and therefore follow the Schottky limit. However, the surface photovoltage saturation values are too low, which is interpreted by an  $n$ -type doping of the interface region due to intercalated metals (Cu, Ag). It seems to us that the layered semiconductors are a special class of material that cannot be described within the usually models of Schottky barrier formation, suggesting that a generalized theory that neglects the special material properties may not exist.

Our results indicate that binding-energy shifts reported in photoemission experiments must be handled with care, as they may also be due to doping profiles induced by the insertion of small quantities of the deposited metal. Photovoltage saturation measurements, especially at low temperatures, principally allow us to discriminate semiconductor band bending from such effects that are not accessible only from the equilibrium binding-energy shift. In general the measurement of nonequilibrium conditions is



more sensitive to deviations of barrier ideality and especially important for solar cell application and should be more thoroughly elaborated and included in UHV studies of semiconductor junctions. Additional experiments, especially at low temperatures and with other metals, are planned to further clarify this point.

#### ACKNOWLEDGMENTS

We thank H. Sehnert for his technical assistance in performing this work and Professor H. Tributsch for helpful discussions and friendly support. This work was funded in part by a grant of the Bundesminister für Forschung und Technologie (BMFT).

\*Permanent address: E. I. DuPont de Nemours & Co., Experimental Station, Wilmington, DE 19898.

<sup>1</sup>E. H. Rhoderick and R. H. Williams, *Metal-Semiconductor Contacts*, 2nd ed. (Oxford Science Publishers, Oxford, 1988).

<sup>2</sup>*Metal Semiconductor Schottky Barrier Junctions and Their Applications*, edited by B. L. Sharma (Plenum, New York, 1984).

<sup>3</sup>L. J. Brillson, *Surf. Sci. Rep.* **2**, 1 (1982).

<sup>4</sup>W. Schottky, *Z. Phys.* **113**, 467 (1939); **118**, 539 (1942).

<sup>5</sup>J. Bardeen, *Phys. Rev.* **71**, 717 (1947).

<sup>6</sup>S. Kurtin, T. C. McGill, and C. A. Mead, *Phys. Rev. Lett.* **22**, 1433 (1969).

<sup>7</sup>M. Schlüter, *Phys. Rev. B* **17**, 5044 (1978).

<sup>8</sup>A. Hiraki, *Surf. Sci.* **168**, 74 (1986).

<sup>9</sup>W. E. Spicer, T. Kendelewicz, N. Newman, K. K. Chin, and I. Lindau, *Surf. Sci.* **168**, 240 (1986).

<sup>10</sup>W. E. Spicer, T. Kendelewicz, N. Newman, R. Cao, C. McCants, K. Miyano, I. Lindau, Z. Liliental-Weber, and E. R. Weber, *Appl. Surf. Sci.* **33/34**, 1009 (1988).

<sup>11</sup>V. Heine, *Phys. Rev.* **138**, A1689 (1965).

<sup>12</sup>S. G. Louie, J. R. Chelikowski, and M. L. Cohen, *Phys. Rev. B* **15**, 2154 (1977).

<sup>13</sup>J. Tersoff, *Phys. Rev. Lett.* **52**, 465 (1984); *Phys. Rev. B* **30**, 4874 (1984).

<sup>14</sup>R. Ludeke, D. Straub, F. J. Himpsel, and G. Landgren, *J. Vac. Sci. Technol. A* **4**, 874 (1986).

<sup>15</sup>L. J. Brillson, *J. Vac. Sci. Technol.* **20**, 652 (1982); L. J. Brillson, C. F. Brucker, A. D. Katnani, N. G. Stoffel, R. Daniels, and G. Margaritondo, *Surf. Sci.* **132**, 212 (1982).

<sup>16</sup>W. Mönch, *Phys. Rev. Lett.* **58**, 1260 (1987).

<sup>17</sup>W. Mönch, *Festkörperprobleme (Advances in Solid State Physics)*, edited by P. Grosse (Pergamon, Braunschweig, 1986), Vol. XXVI, p. 67.

<sup>18</sup>W. Jaegermann, *Chem. Phys. Lett.* **126**, 301 (1986); *Ber. Bunsenges. Phys. Chem.* **92**, 1261 (1988).

<sup>19</sup>J. L. Stickney, S. D. Rosasco, B. C. Schardt, T. Solomun, A. T. Hubbard, and B. A. Parkinson, *Surf. Sci.* **136**, 15 (1984).

<sup>20</sup>M. Salmeron, G. A. Somorjai, A. Wold, R. Chianelli, and K. S. Liang, *Chem. Phys. Lett.* **90**, 105 (1982).

<sup>21</sup>G. J. Hughes, A. McKinley, R. H. Williams, and I. T. McGovern, *J. Phys. C* **15**, L159 (1982); R. H. Williams, A. McKinley, G. J. Hughes, V. Montgomery, and I. T. McGovern, *J. Vac. Sci. Technol.* **21**, 594 (1982).

<sup>22</sup>T. Tambo and C. Tatsuyama, *Surf. Sci.* **222**, 332 (1989); **222**, 342 (1989).

<sup>23</sup>X. Zaoui, R. Mamy, and A. Chevy, *Surf. Sci.* **204**, 174 (1988).

<sup>24</sup>I. T. McGovern, E. Dietz, H. H. Rotermund, A. M. Bradshaw, W. Braun, W. Radlik, and J. F. McGilp, *Surf. Sci.* **152/153**, 1203 (1985).

<sup>25</sup>J. R. Lince, D. J. Carré, and P. D. Fleischauer, *Langmuir* **2**, 805 (1986); *Phys. Rev. B* **36**, 1647 (1987).

<sup>26</sup>F. S. Ohuchi, W. Jaegermann, and B. A. Parkinson, *Surf. Sci.* **194**, L69 (1988); W. Jaegermann, F. S. Ohuchi, and B. A. Parkinson, *Ber. Bunsenges. Phys. Chem.* **93**, 29 (1989).

<sup>27</sup>W. Jaegermann, F. S. Ohuchi, and B. A. Parkinson, *Surf. In-*

*terf. Anal.* **12**, 293 (1988); W. Jaegermann, F. S. Ohuchi, and B. A. Parkinson, *Surf. Sci.* **201**, 211 (1988).

<sup>28</sup>J. R. Lince, T. B. Stewart, P. D. Fleischauer, J. A. Yarmoff, and A. Taleb-Ibrahimi, *J. Vac. Sci. Technol. A* **7**, 2469 (1989); J. R. Lince, T. B. Stewart, M. M. Hills, P. D. Fleischauer, J. A. Yarmoff, and A. Taleb-Ibrahimi, *Surf. Sci.* **223**, 65 (1989).

<sup>29</sup>S. Kennou, S. Ladas, and C. Papageorgopoulos, *Surf. Sci.* **152/153**, 1213 (1985); S. Ladas, S. Kennou, M. Karamatos, S. D. Foulis, and C. Papageorgopoulos, *ibid.* **189/190**, 261 (1987); M. Karamatos and C. Papageorgopoulos, *ibid.* **160**, 451 (1985); *Appl. Surf. Sci.* **29**, 279 (1987).

<sup>30</sup>F. S. Ohuchi, W. Jaegermann, C. Pettenkofer, and B. A. Parkinson, *Langmuir* **5**, 439 (1989).

<sup>31</sup>M. I. Johnson, H. I. Starnberg, and H. P. Hughes, *Surf. Sci.* **178**, 290 (1986); H. I. Starnberg and H. P. Hughes, *J. Phys. C* **20**, 4429 (1987).

<sup>32</sup>F. R. Gamble, *J. Solid State Chem.* **9**, 358 (1974).

<sup>33</sup>C. Clemen, X. I. Saldana, P. Munz, and E. Bucher, *Phys. Status Solidi A* **49**, 437 (1978).

<sup>34</sup>B. A. Parkinson, following procedures outlined in *J. Electroanal. Chem.* **334**, 133 (1987).

<sup>35</sup>J. E. Demuth, W. J. Thompson, N. J. DiNardo, and R. Imbuhl, *Phys. Rev. Lett.* **126**, 301 (1986).

<sup>36</sup>J. H. Scofield, *J. Electron Spectrosc.* **8**, 129 (1976).

<sup>37</sup>P. M. Williams, in *Physics and Chemistry of Materials with Layered Structure, Vol. 4: Optical and Electrical Properties*, edited by P. A. Lee (Reidel, Dordrecht, 1976); G. Margaritondo, in *Electronic Structure and Electronic Transitions in Layered Materials*, edited by V. Grasso (Reidel, Dordrecht, 1986).

<sup>38</sup>R. Coehoorn, C. Haas, J. Dijkstra, C. J. Flipse, R. A. de Groot, and A. Wold, *Phys. Rev. B* **35**, 6195 (1987).

<sup>39</sup>W. Jaegermann, C. Pettenkofer, and B. A. Parkinson, *Vacuum* (to be published).

<sup>40</sup>P. Heimann, H. Neddermeyer, and H. F. Roloff, *J. Phys. C* **10**, L17 (1977); T. E. Felter, W. H. Weinberg, P. A. Zhdan, and G. K. Boreskov, *Surf. Sci.* **97**, L313 (1980).

<sup>41</sup>G. E. Rhead, M. G. Barthès, and C. Argile, *Thin Solid Films* **82**, 201 (1981).

<sup>42</sup>D. L. Doering, F. S. Ohuchi, W. Jaegermann, and B. A. Parkinson, in *Epitaxy of Semiconductor Layered Structures*, Vol. 102 of *Materials Research Society Symposium Proceedings*, edited by R. T. Tung, L. R. Dawson, and R. L. Gunsher (MRS, Pittsburgh, 1988); p. 4141; M. L. Bortz, F. S. Ohuchi, and P. A. Parkinson, *Surf. Sci.* **223**, 285 (1989).

<sup>43</sup>K. Kam and B. A. Parkinson, *J. Phys. Chem.* **86**, 463 (1982).

<sup>44</sup>A. Klein, C. Pettenkofer, and W. Jaegermann, unpublished.

<sup>45</sup>C. A. Koval, J. B. Olson, and B. A. Parkinson, *ACS Symposium Series* **378**, 438 (1988).

<sup>46</sup>S. Trasatti, *J. Electroanal. Chem.* **209**, 417 (1986); W. N. Hansen and D. M. Kolb, *ibid.* **100**, 493 (1979).

<sup>47</sup>A. Klein, C. Pettenkofer, and W. Jaegermann, unpublished.

<sup>48</sup>*CRC Handbook of Chemistry and Physics*, 67th ed., edited by R. C. Weast (CRC Press, Cleveland, 1986).

- <sup>49</sup>S. M. Sze, *Physics of Semiconductor Devices* (Wiley, New York, 1981).
- <sup>50</sup>W. E. Spicer, S. Eglash, I. Lindau, C. Y. Su, and P. R. Skeath, *Thin Solid Films* **89**, 447 (1982); L. J. Brillson, *ibid.* **89**, L27 (1982); S. Eglash, W. E. Spicer, and I. Lindau, *ibid.* **89**, L35 (1982).
- <sup>51</sup>J. Gobrecht, H. Gerischer, and H. Tributsch, *Ber. Bunsenges. Phys. Chem.* **82**, 1331 (1978).
- <sup>52</sup>*Physics and Chemistry of Materials with Layered Structure, Vol. 6; Intercalated Layered Material*, edited by F. Levy (Reidel, Dordrecht, 1979).
- <sup>53</sup>H. P. Schweikardt, M. Ch. Lux-Steiner, M. Vögt, and E. Bucher, *20th IEEE Photovoltaic Specialists Conference, Las Vegas, 1988* (IEEE, New York, 1988).
- <sup>54</sup>C. Pettenkofer and W. Jaegermann, unpublished.
- <sup>55</sup>A. Schellenberger, R. Schlaf, T. Mayer, E. Holub-Krappe, C. Pettenkofer, W. Jaegermann, U. A. Ditzinger, and H. Neddermeyer, unpublished.